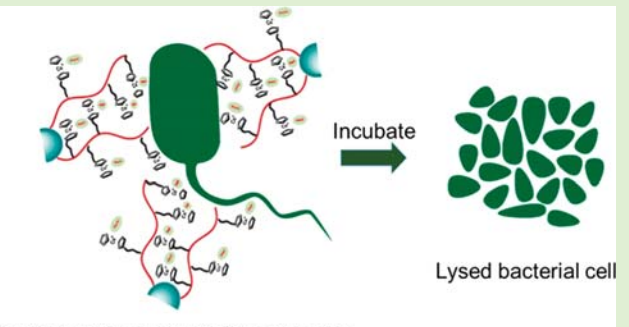
Charged Metallopolymer-Grafted Silica Nanoparticles for **Antimicrobial Applications**

Parasmani Pageni, † Peng Yang, † Yung Pin Chen, Yucheng Huang, † Marpe Bam, † Tianyu Zhu, † Mitzi Nagarkatti, † Brian C. Benicewicz, † Alan W. Decho, and Chuanbing Tang*, †

Supporting Information

ABSTRACT: Inappropriate and frequent use of antibiotics has led to the development of antibiotic-resistant bacteria, which cause infectious diseases that are difficult to treat. With the rising threat of antibiotic resistance, the need to develop effective new antimicrobial agents is prominent. We report antimicrobial metallopolymer nanoparticles, which were prepared by surface-initiated reversible addition-fragmentation chain transfer polymerization of a cobaltoceniumcontaining methacrylate monomer from silica nanoparticles. These particles are capable of forming a complex with β -lactam antibiotics, such as penicillin, rejuvenating the bactericidal activity of the antibiotic. Disk diffusion assays showed significantly increased antibacterial activities against both



Bacteria with nanoparticle conjugates

Gram-positive and Gram-negative bacteria. The improved efficiencies were attributed to the inhibition of hydrolysis of the β lactam antibiotics and enhancement of local antibiotics concentration on a nanoparticle surface. In addition, hemolysis evaluations demonstrated minimal toxicity to red blood cells.

INTRODUCTION

The widespread and excessive use of antimicrobial drugs has increased the endurance of microbes, making them more tolerant toward conventional antibiotics. Antimicrobial resistance has been highlighted as "one of the greatest threats to human health worldwide" by the Infectious Diseases Society of America, and the White House announced the National Strategy for Combating Antibiotic-Resistant Bacteria (CARB). According to U.S. Centers for Disease Control and Prevention, at least 2 million people are affected annually by drug-resistant bacteria in the U.S. alone, and 23,000 of them lose their lives.² The burden created by these infections on the economy is also substantial and is estimated to result in \$20 billion in additional health care costs and \$35 billion in lost productivity annually.³ As a result of antibiotic resistance, it is hard to treat major diseases because the drugs used are becoming progressively less effective. A variety of antibiotics are now being labeled ineffective, and the proliferation of bacteria is surging. The growing need to develop powerful antibacterial agents is fueled by the increasing daily incidence of bacterial infections. Therefore, it is urgent to direct efforts toward the development of novel antibiotics and more-effective therapeutic strategies to tackle this escalating health crisis.

The predominant synthetic microbial agents are compounds or polymers having cationic groups like quaternary ammonium

or phosphonium, which promote rapid adsorption onto the negatively charged bacterial cell surfaces. 4-8 Because of the physical nature of membrane disruption, the possibility of developing new resistant strains is reduced significantly. However, many of these antimicrobial agents, although effective against certain types of bacterial strains, are notoriously toxic toward mammalian cells, thus limiting their roles in battling infections. 9-13 The use of nanotechnology has often been considered in developing alternative antimicrobial therapies. Nanoparticles have been widely used in pharmaceuticals, biomedicine, and microbiology. 14,15 Nanoparticles could be a powerful tool to combat bacterial infections. 16 Antimicrobial agents have been constructed by both organic and inorganic nanoparticles such as silver, ^{17–19} gold, ^{20–22} zinc oxide, ^{23,24} titanium dioxide, ^{25,26} silica, ^{27,28} copper oxide, ²⁹ magnesium oxide, ³⁰ carbon-based nanoparticles such as carbon nanotubes,^{31–33} fullerenes,³⁴ and graphene oxide.³⁵ In particular, silica nanoparticles have a high chemical, thermal, and colloidal stability and have been found to be useful in biomedical applications due to their biocompatibility, low toxicity, low density, capacity for encapsulation, and easy synthesis. ^{36,37} In

Received: October 23, 2017 Revised: January 10, 2018 Published: January 31, 2018

[†]Department of Chemistry and Biochemistry and *Department of Environmental Health Sciences, University of South Carolina, Columbia, South Carolina 29208, United States

Department of Pathology, Microbiology and Immunology, University of South Carolina, School of Medicine, Columbia, South Carolina 29209, United States

addition, they have larger surface areas that can be functionalized using organosilane chemistry to introduce desirable functional groups to regulate drug loading. The bactericidal effect of silica nanostructures could be fine-tuned by adjusting various parameters like particle size, shape, porosity, and surface functionalization.³⁸ Kim et al. synthesized dual mode silica nanoparticles for specific binding to his-tagged proteins for purification and labeling of proteins.³⁹ Bharali et al. used aminosurface-functionalized plasmid DNA-bound silica nanoparticles for in vivo gene delivery. 40 Liu et al. and others broadened dimensions of silica nanoparticles to enhance image contrast and reported a detectable ultrasound behavior after administering 100 nm solid silica nanoparticles into mice. 41,42 A new class of nanoparticles, polymeric nanoparticles, has been touted for various biomedical applications due to the versatility in modification to incorporate different functionalities. 15,43-45 Nederberg et al. synthesized polymeric nanoparticles consisting of cationic amphiphilic triblock polycarbonates that selectively lysed microbial membranes. 46 They were not only biodegradable but also in vivo applicable and highly effective against drugresistant bacteria.

We recently demonstrated that low cytotoxic cationic cobaltocenium metallopolymers have antimicrobial efficacy against various bacterial strains including multidrug-resistant bacteria by disarming activities of β -lactamase. These charged metallopolymers were capable of protecting conjugated antibiotics via ion-pairing with cobaltocenium. We showed that these metallopolymers can inhibit the detrimental effects of the β -lactamase enzyme that is responsible for the hydrolysis of β -lactam antibiotics.

In an effort to further enhance the efficacy of cobaltocenium polymers, we report herein surface-grafted cobaltocenium-containing silica nanoparticles. We carried out surface-initiated reversible addition—fragmentation chain transfer (RAFT) polymerization of a cobaltocenium-containing methacrylate monomer from silica nanoparticles coated with 4-cyanopentanoic acid dithiobenzoate (CPDB). We then conjugated the antibiotic penicillin-G with the nanoparticles by ion-pairing between the cationic cobaltocenium moiety in the nanoparticles and carboxylate anions of antibiotics. Such bioconjugated nanoparticles not only reduced the activity of β -lactamase but effectively lysed both Gram-positive and Gram-negative bacterial cells.

■ EXPERIMENTAL SECTION

Characterization. ¹H (400 MHz), ¹³C (100 MHz), and ¹⁹F (376 MHz) NMR spectra were recorded on a Varian Mercury 400 NMR spectrometer with tetramethylsilane (TMS) as an internal reference. Mass spectrometry was conducted on a Waters Micromass Q-TOF mass spectrometer, and the ionization source was positive ion electrospray. UV-vis absorbance was carried out on a Shimadzu UV-2450 spectrophotometer with a 10.00 mm quartz cuvette and monochromatic light of various wavelengths over a range of 190-900 nm. A Hitachi 8000 transmission electron microscope (TEM) was used to acquire images at an operating voltage of 150 kV. TEM samples were prepared by dropping a solution of nanoparticles on carbon-supported copper grids and then dried before observation. Dynamic light scattering (DLS) was operated on a Nano-ZS instrument, Model ZEN 3600 (Malvern Instruments). Field-emission scanning electron microscopy (FE-SEM, Zeiss UltraPlus) was used for imaging of bacterial cells after overnight incubations with test drugs. The samples were first coated for 45 s with gold using a Denton Dest II Sputter Coater then observed by SEM.

Materials and Methods. 2-Cobaltoceniumamidoethyl methacrylate hexafluorophosphate (CoAEMAPF₆) was synthesized according

to our earlier report.⁴⁹ 2-Aminoethyl methacrylate hydrochloride (90%), N-(3-(dimethylamino)propyl)-N'-ethylcarbodiimide hydrochloride (EDC-HCl, 98%), 4-(dimethylamino) pyridine, and tetrabutylammonium chloride (TBACl) were purchased from Aldrich and used as received. Water was from Thermo Scientific Nanopure with ion conductivity at 18.2 M Ω . The following bacterial strains were purchased from ATCC: Staphylococcus aureus (ATCC-33591), Escherichia coli (ATCC-11775), Klebsiella pneumoniae (ATCC-35596), Proteus vulgaris (P. vulgaris, ATCC-33420), and Pseudomonas aeruginosa (ATCC-10145). Nitrocefin was purchased from TOKU-E and used as received. The sodium salt of penicillin-G was purchased from VWR and used as received. 4-Cyanopentanoic acid dithiobenzoate (CPDB) was obtained from Strem Chemical Inc. CPDBimmobilized silica nanoparticles were synthesized according to the literature. 50 Azobis (isobutyronitrile) (AIBN) was recrystallized from methanol before use. All other chemicals were from commercial sources and used as received.

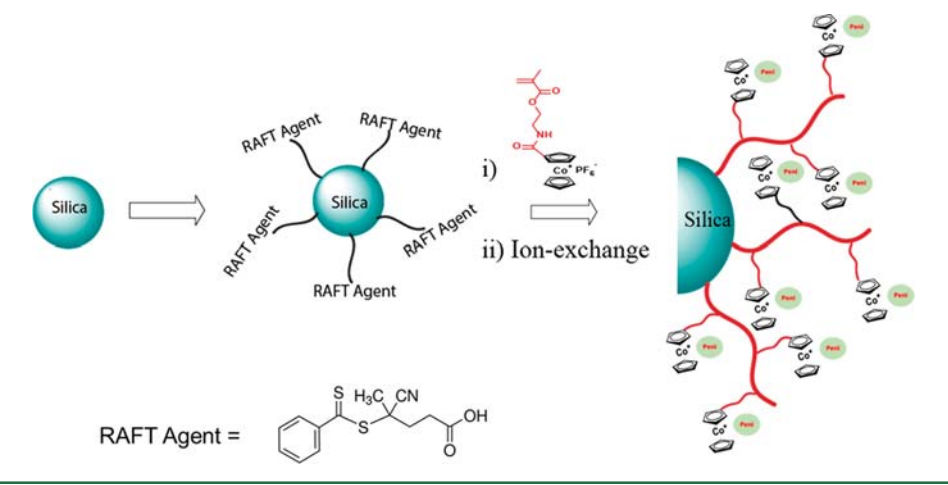
Synthesis of Cobaltocenium-Containing Silica Nanoparticles. CoAEMAPF₆ (200 mg, 0.41 mmol) CPDB-coated silica nanoparticles (69.5 mg, 59 $\mu mol/g$, 1 mmol) and 0.4 mL of dry dimethyformamide (DMF) were added to a 10 mL Schlenk tube. To ensure adequate dispersion of silica nanoparticles, the solution was sonicated for 5 min, and AIBN (0.2 mg, 1.23 $\mu mol)$ was added. The resulting solution was degassed by purging nitrogen for 30 min and then placed in an oil bath of 90 °C until the desired conversion was reached. The polymerization was quenched by opening to air and cooling with ice water. The reaction mixture was precipitated in cold dichloromethane three times and vacuum-dried. Ion-exchange to Clwas performed according to a previous report using tetrabutylammonium chloride salt (TBACI). ⁵¹ A typical procedure was as follows: 1 mL of PF₆-paired CsNP (30 mg/mL in acetonitrile) was slowly dropped into 5 mL of TBACl solution (in acetonitrile) under vigorous stirring. After stirring for 5 min, the precipitated Cl⁻-paired CsNP was collected and washed by acetonitrile three times to remove PF₆ anions and excess TBACl. The solid yellow CsNP-Cl was then vacuum-dried and collected. The polymer chains were cleaved using HF, and NMR was performed on the cleaved polymer chains.

Synthesis of CsNP-Penicillin Bioconjugates. Cobaltocenium-containing silica nanoparticles with Cl⁻ and penicillin-G sodium salt were initially dissolved in deionized water (1 mL) with molar ratios (penicillin salt to cobaltocenium moieties) in the range of 1.05 to 1.15. The solution was stirred for 2 h and then dialyzed against 3 L of deionized water for 9 h. The solution in a dialysis bag was collected and freeze-dried. The CsNP-Peni conjugates were obtained as a yellow powder.

Growth of Bacteria. The antibacterial activity of cobaltoceniumcontaining silica nanoparticles was evaluated using standard diskdiffusion assays (ASTM: the Kirby Bauer diffusion test). First, actively growing cultures of each bacterial strain, previously grown on Mannitol salt agar (MSA), were inoculated on tryptic soy broth (TSB) agar plates. A subsample (10 μ L) of each bacterial culture (cell concentrations were 1.0×10^6 CFU/mL) was diluted to 1 mL in TSB, and 100 μ L of cell culture was spread on TSB agar plates to form a bacterial lawn covering the plate surface. Then, a 6 mm filter disc was laid on the agar surface to which the nanoparticle solution was added at the desired concentration. All plates were incubated overnight at 37 °C. The development of a clear zone around the disk was indicative of the ability of antimicrobial drugs to kill bacteria. By quantifying the area of inhibition (knowing its diameter and the depth of the agar), a minimum inhibitory concentration (MIC) was calculated for each material/bacterial combination using established protocols. 52

Bacterial Morphology by FE-SEM. Field-emission scanning electron microscopy (FE-SEM) was used to examine changes in the morphology of bacterial cells after incubations with test drugs. In summary, 20 μ L of bacterial cell solutions were grown on glass slides in a 6-well plate containing 2 mL of TSB medium at 37 °C overnight. Cell suspensions were diluted to OD₆₀₀ = 1.0. After adding predetermined amounts of test drugs to the 1 mL cell stock solution, they were incubated overnight at 37 °C. A cell suspension without any chemicals was used as the control. The samples were then fixed in

Scheme 1. Synthesis of Cobaltocenium-Containing Silica Nanoparticles by Surface-Initiated RAFT Polymerization



cacodylate buffer with 2.5% glutaraldehyde solution (pH 7.2) for 2-3 h at 4 °C and postfixed with 1% osmium tetraoxide at 4 °C for 1 h. Samples were dehydrated under a critical point and then coated with gold using a Denton Dest II Sputter Coater for 120 s and observed by FE-SEM.

LIVE/DEAD Bacterial Viability Assays. The five bacterial strains were inoculated and prepared by a similar procedure as mentioned above. One mL of active bacterial stock solution was introduced to 5 μ g penicillin solutions. An untreated cell suspension was used as the control. Following overnight incubation at 37 °C, 1 μ L LIVE/DEAD BacLight (Bacterial Viability Kit; Invitrogen Inc.) was added to the incubation solution. After incubation for 15 min, cells were imaged using a Leica TCS SP5 laser scanning confocal microscope with a 63× oil immersion lens. When excited at 488 nm with argon and helium/neon lasers, bacteria with intact membranes display green fluorescence (emission = 500 nm) and bacteria with disrupted membranes fluoresced red (emission = 635 nm).

Drug Resistance Study. At first, a 50 μ L aqueous solution of CsNP-penicillin conjugates with half of the MIC concentration were added to 96-well plates. Then, 150 μ L bacterial TSB solutions (OD₆₀₀ = 1.00) were added to the wells. The bacterial TSB solution without conjugates was used as the control. The assay plate was incubated at 37 °C until the bacteria were grown to an optical density of ~1.00 (OD₆₀₀ = ~1.00) in control samples. All assays were carried out in duplicate in the same assay plate. The experiment was repeated for 15 passages.

Effects of CsNP Copolymers on β -Lactamase Activity. Nitrocefin (50 μ L, 1.0 μ g/mL DMSO solution) and CsNP with different concentrations (100, 200, and 400 μ g) were added to 1 mL of H₂O and stirred for 12 h. Then, 1 μ L of β -lactamase PBS buffer solution (0.1 μ g/mL, determined by Biorad Protein Assay) was added to the above solution. A solution without nanoparticles was used as a control. After 1 h, the β -lactamase activity was measured by UV—vis absorbance at 480 nm.

Hemolysis Evaluation for Cytotoxicity Determination. Blood was collected from mice in heparinized tubes and diluted by mixing 800 μ L of blood with 1000 μ L of PBS. Nanoparticle samples were prepared in PBS at concentrations of 10, 50, 100, and 500 μ g/mL and 60 μ L of the diluted blood samples was added to 3 mL of the nanoparticle conjugates, PBS, or 0.1% Triton-X100 in PBS. The samples were incubated for 1 h at 37 °C followed by centrifugation for 10 min at 1500 rpm. Supernatants were collected, and OD was measured at 545 nm to calculate the hemolysis rate using the formula HR = (AS – AN)/(AP – AN), where AS, AN, and AP are OD values of the supernatants from test samples, negative control (PBS), and positive control (0.1% Triton-X100), respectively.

■ RESULTS AND DISCUSSION

1. Synthesis of Cobaltocenium-Containing Silica Nanoparticles. The cobaltocenium-containing silica nanoparticles (CsNP) were prepared via RAFT polymerization using 2-cobaltocenium amidoethyl methacrylate hexafluorophosphate (CoAEMAPF₆) as a monomer and AIBN as an initiator, mediated by CPDB-coated silica nanoparticles in DMF at 90 °C (Scheme 1 and Scheme S1). We previously synthesized a cobaltocenium methacrylate monomer with ester and amide linkers for various applications and studies. S3-55 A similar procedure was followed to synthesize CoAEMAPF₆ by reacting cobaltocenium monoacid with 2-aminoethyl methacrylate hydrochloride in the presence of coupling agent *N*-(3-(dimethylamino)propyl)-*N'*-ethylcarbodiimide (EDC).

RAFT polymerization has been demonstrated to provide quantitative and precise control over the molecular weight. 56-5 We carried out RAFT polymerization by exploiting a "grafting from" technique. 50,59-61 The silane surface chemistry was used to treat the colloidal silica nanoparticles with 3-aminopropyldimethylethoxysilane followed by the amidation reaction between amino groups and the CPDB RAFT agent. The amount of RAFT agent anchored onto the modified silica nanoparticles was determined quantitatively by comparing the absorption at ~303 nm for the CPDP-anchored silica nanoparticles to a standard absorption curve made from known amounts of the free CPDB (Figure S1). Three different types of silica nanoparticles were synthesized by differing various grafting densities from 0.084 to 0.481 chain/nm² (20, 59, and 114 μ mol/g CPDB). Most likely, these grafting densities were significantly below the maximum grafting density of CPDB that could be allowed (typically close to 1.0 chain/ nm²). The disappearance of the vinyl protons from methacrylate around 6.2 and 5.6 ppm and the appearance of broad peaks around 0.5-2.0 ppm in the ¹H NMR spectrum suggested the successful polymerization. (Figure S2). The molecular weight was controlled by tracking the conversion during the polymerization process using NMR. The polymers were obtained with the degree of polymerization in the range of 26-28. The targeted molecular weight was in the range of 12000-15000 g/mol, which displayed strong antibacterial properties based on our previous studies (Table 1).⁴⁷ The nanoparticles were further characterized by FTIR and EDX elemental analysis to confirm the presence of major bonds and elements in the nanoparticles (Figures S3 and S4).

Biomacromolecules

Table 1. Cobaltocenium-Containing Silica Nanoparticles and Their Characterization

entry	total surface density a (μ mol/g)	total surface density (chain/nm²)	$M_{\rm n}^{b}$ (g/mol)	diameter ^c (nm)	zeta potential ^d (mV)
CsNP 1	20	0.084	12700	48	40.4
CsNP 2	59	0.249	13700	50	55.1
CsNP 3	114	0.481	13200	51	62.6

"Equivalent of CPDB. $^bM_{\rm n}$ calculated by conversion of CoAEMAPF $_6$ via NMR. c Diameter calculated via DLS. d Zeta potential calculated via DLS.

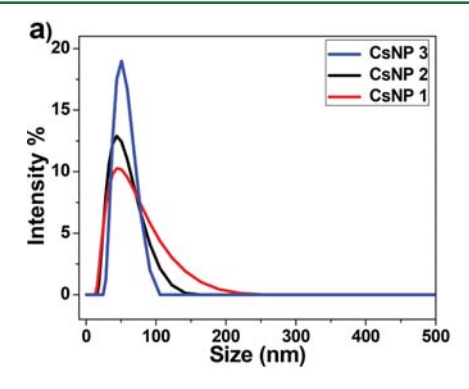
A facile phase-transfer ion-exchange method has been established to prepare hydrophilic cationic cobaltoceniumcontaining polyelectrolytes with diverse counterions using tetrabutylammonium chloride (TBACl) salts.⁵¹ Thus, nanoparticles with PF₆⁻ anions were subjected to anion exchange with TBACl to result in hydrophilic chloride-based particles. The complete conversion from PF₆⁻ to Cl⁻ was confirmed by running ¹⁹F NMR of the resultant nanoparticles (Figure S5). The switch of anions to chloride significantly increased the hydrophilicity of the nanoparticles and facilitated the use of these particles for biomedical applications. The strong electrostatic interaction between the cationic cobaltocenium moieties and stationary phase of microstyragel columns made it difficult to characterize molecular weight by gel permeation chromatography. The nanoparticles were further conjugated with penicillin via ionic interaction between anionic penicillin sodium salt and the cationic cobaltocenium moiety resulting in penicillin-conjugated cobaltocenium-containing silica nanoparticles (CsNP). The excess penicillin salt, which was not complexed with nanoparticles, was removed by dialysis. For convenience, the nanoparticle conjugates were hereafter referred to as CsNP 1 (20 μ mol/g), CsNP 2 (59 μ mol/g), and CsNP 3 (114 μ mol/g).

The mean diameter of cobaltocenium-containing nanoparticles was found to be in the range of 40–50 nm as measured by dynamic light scattering (Figure 1a). The diameter of bare silica nanoparticles was around 20–25 nm, and after polymerization, the mean diameter increased as expected. The average diameter of individual cobaltocenium-containing nanoparticles measured by TEM (Figure 2) was consistent with DLS results. Thermogravimetric analyses (TGA) showed accurate weight loss of nanoparticles with different grafting densities (Figure 1b). To determine the weight percentage of the cobaltocenium, TGA of homopol-

ymers and bare silica nanoparticles were compared with that of cobaltocenium-grafted nanoparticles. On the basis of the TGA measurements, the total weight percentage of cobaltocenium in the nanoparticle in CsNP ranged from 56 to 65 wt %. This information together with ¹H NMR allowed us to calculate the weight percentage of penicillin in the nanoparticles, which was in the range of 28–35 wt %. The equimolar pairing of penicillin with cobaltocenium was confirmed by ¹H NMR by calculating the integration ratio of aromatic peaks ~7.2 ppm from penicillin to the cyclopentadienyl peaks of polymers ~5.5–6.1 ppm (Figure S6).

2. Antimicrobial Activity of Cobaltocenium-Containing Silica Nanoparticles. Antimicrobial susceptibility was determined by the conventional agar disk-diffusion assay following a protocol of Kirby Bauer diffusion test. 62 Staphylococcus aureus and Escherichia coli were chosen as representative Gram-positive and Gram-negative bacteria, respectively. For the effective optimal concentration to be determined, three different amounts of penicillin (4, 6, and 8 μ g) were tested against the two bacterial strains as shown in Figure S7. While carrying out the disk-diffusion assays, concentrations of penicillin were kept constant in both nanoparticle treatments and controls. The optimal activity was obtained with 6 μ g of penicillin and used throughout the tests. The ability of the complex to kill the bacteria was represented by the development of a clear zone around the disk also known as the inhibition zone. Higher inhibition zones were seen in for the Gram-positive S. aureus in comparison to that of the Gram-negative E. coli. The additional outer polysaccharide layer in the Gram-negative bacteria might have acted as an extra layer of shielding for the test drugs to penetrate, resulting in the smaller inhibition zone. 62

For further investigation of Gram-negative bacteria, tests were extended to the following bacteria using the above-mentioned protocol: *Pseudomonas aeruginosa, Proteus vulgaris,* and *Klebsiella pneumonia.* Among them, *P. aeruginosa, K. pneumonia,* and *S. aureus* are among the six pathogens in a class "ESKAPE" termed by the CDC that can evade the influence of antibiotics and develop resistance. As shown in Figure 3 and Figure S8, penicillin-G alone showed minimal antibacterial efficacy at a given concentration when compared to the CsNP bioconjugates. In the case of *S. aureus,* the inhibition zone caused by penicillin was 9 mm, whereas the zones created by CsNP-penicillin conjugates were much larger at ~19 mm. The amount of cobaltocenium in the control CsNP-Cl was probably too low for observing the onset of any antimicrobial activity.



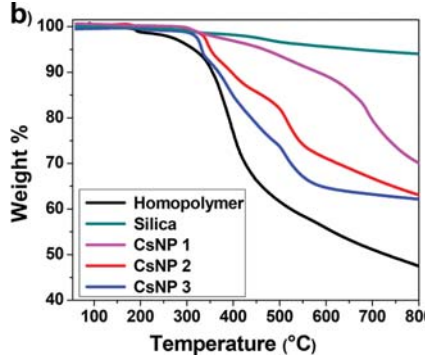


Figure 1. (a) Dynamic light scattering measurements showing nanoparticle sizes and (b) thermogravimetric analysis of cobaltocenium-containing silica nanoparticles.

Biomacromolecules

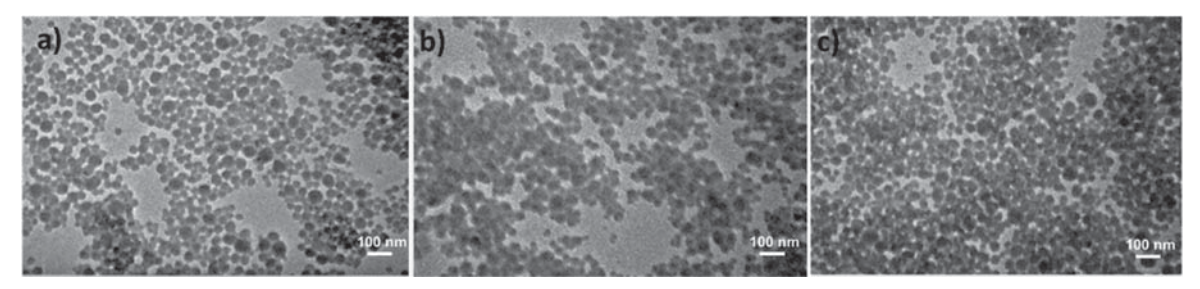


Figure 2. TEM images of nanoparticles for (a) CsNP 1, (b) CsNP 2, and (c) CsNP 3.

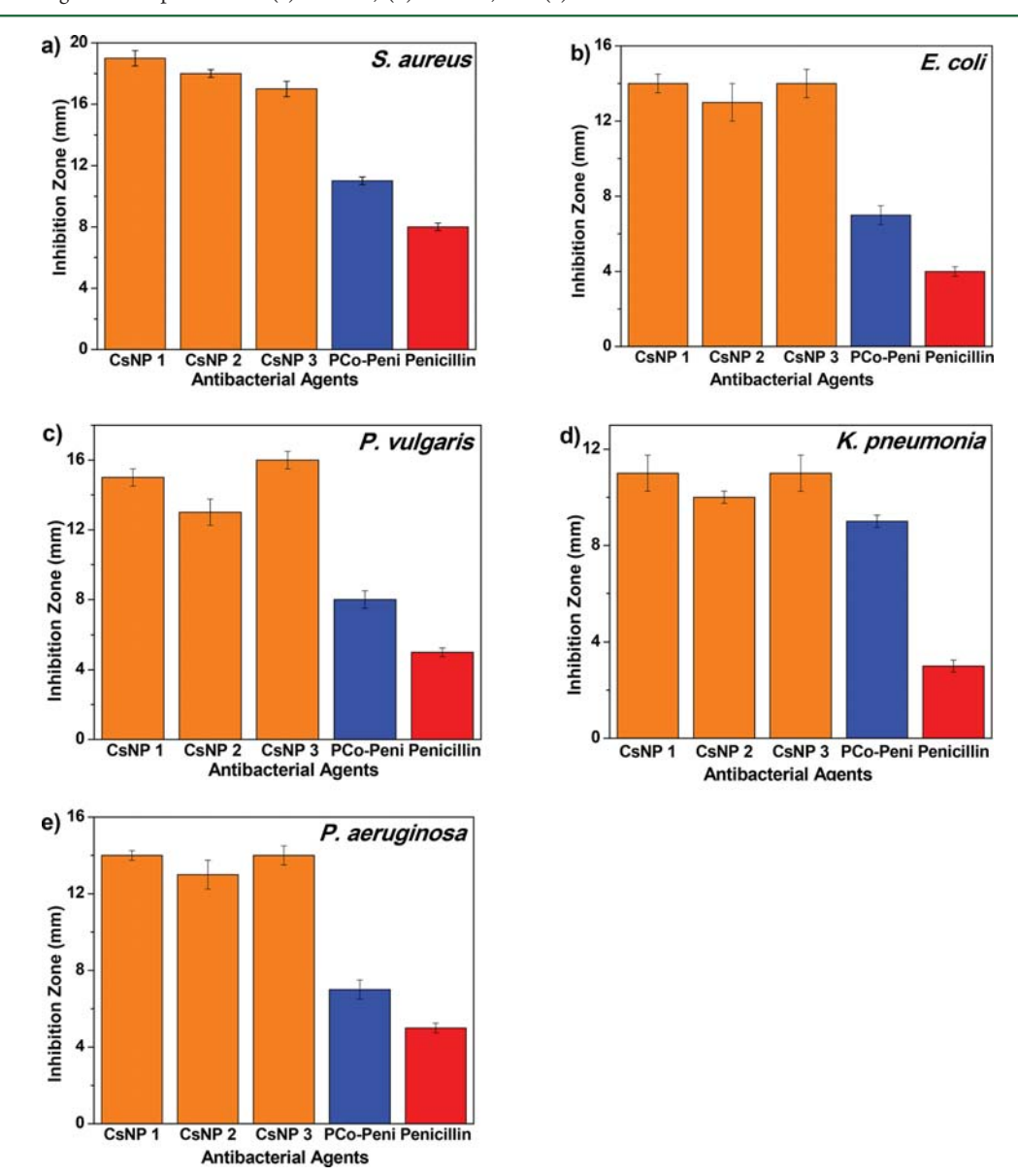


Figure 3. Inhibition zones of CsNP-Peni conjugates against various strains of bacteria at 6 μ g penicillin-G/disk using disk-diffusion assays: (a) S. aureus, (b) E. coli, (c) P. vulgaris, (d) K. pneumonia, and (e) P. aeruginosa.

The inhibition zone caused by homopolymer conjugate (PCo-Peni) was 12 mm, which was larger than that of penicillin alone but still smaller than those observed for nanoparticle-penicillin conjugates. All three CsNP-penicillin conjugates resulted in bigger inhibition zones than those of penicillin, CsNP-Cl nanoparticles, and the homopolymer-penicillin conjugate.

The results presented above demonstrate the synergistic effects of the cobaltocenium-penicillin complex in protecting the antibiotics, leading to increased lysis of bacterial cells. This led us to believe that CsNP-penicillin conjugates could be upgraded ammunition from the currently known homopolymer-penicillin conjugate in combating bacterial infections. The

CsNP conjugates have a greater charge density of cationic cobaltocenium on the surface, which provides an advantage for higher bactericidal efficacy when compared to those of the individual polymers. Even though the grafting densities of the nanoparticles were different, the inhibition zones caused by the nanoparticle conjugates were similar. This could be attributed to the similar sizes of nanoparticle conjugates resulting in a similar zone of diffusion in the agar gel. The diameters of nanoparticles were very close to each other; thus, we predict that similar diffusion likely occurred in the agar gel, leading to the similar antimicrobial activities observed.

Minimum inhibitory concentrations were calculated for each material/bacterial combination using the established protocol and are given in Table 2.⁵² The mean MIC of CsNPs against

Table 2. Minimum Inhibitory Concentrations (MICs) of Different Antimicrobial Agents against Five Strains of Bacteria

	minimum inhibitory concentration (MIC, $\mu g/mL$)						
compd	S. aureus	E. coli	P. vulgaris	P. aeruginosa	K. pneumonia		
CsNP 1	3.03	5.57	5.42	5.57	10.92		
CsNP 2	3.78	7.58	5.91	6.46	9.90		
CsNP 3	2.73	4.85	5.20	5.57	10.10		
penicillin	13.48	17.06	17.50	19.41	26.66		

Gram-positive strain *S. aureus* was 3.18 \pm 0.54 μ g/mL, which was ~4-times lower than that of penicillin at 13.48 μ g/mL. Similarly, for Gram-negative strains, the MIC values of CsNPs followed a similar trend and were much lower than that of penicillin alone. Compared with penicillin alone, nanoparticle-polymer conjugates displayed significantly higher efficacies against both Gram-positive and Gram-negative strains.

The increased bactericidal effectiveness was further supported by qualitative observations using confocal scanning laser microscopy (CSLM) studies (Figure 4). LIVE/DEAD bacteria viability assays using CSLM indicated greater levels of cell death and lower cell densities when bacterial cells were exposed to CsNP-Peni conjugates. Most of the cells exposed to penicillin alone exhibited primarily green fluorescence indicating live

cells, whereas cells incubated with CsNP-Peni bioconjugates displayed primarily red or yellow fluorescence, indicating cell death. Furthermore, SEM imaging was used to compare differences in morphology before and after treatment with CsNP-Peni conjugates (Figure 5). Control samples contained intact bacterial cells with smooth surfaces, whereas the cells incubated with conjugates were significantly damaged with obvious disruptions in the original morphology. The collapsed cell envelopes of the incubated bacterial cells marked the physical damage of cell membranes.

The Nitrocefin assay, in conjunction with UV–vis spectrophotometry, was used to observe the effects of CsNP on β -lactamase activity (Figure S9). The original yellow color of controls of a nitrocefin solution changed to red within a few minutes after the addition of β -lactamase. The change in color was the result of hydrolysis of the β -lactam ring of antibiotics and can be observed by an absorption peak near 480 nm (Figure S9b). When nitrocefin was complexed with CsNP, there was a minimal change in color, implying protection of the β -lactam ring by the cobaltocenium moiety complex. When a higher concentration of CsNP was used, the color of the yellow solution remained unchanged. This was interpreted as complete shutdown of the β -lactamase activity against β -lactam antibiotics.

For evaluating the probability of the CsNP-penicillin conjugates to induce resistance in bacteria, a drug resistance study was conducted for the most potent nanoparticle conjugate, CsNP 3 (lowest MIC), against both Gram-positive and Gram-negative bacteria. As shown in Figure 6, the OD_{600} values of the nanoparticle conjugates remain virtually constant even after 15 consecutive passages against both *S. aureus* and *E. coli*, indicating that the bacteria did not readily develop resistance toward the nanoparticle conjugate.

The improved bactericidal efficiencies of CsNP-penicillin conjugates could be attributed to the enhanced local concentration of the cobaltocenium-penicillin complex on the nanoparticle surface. Most of the antibacterial agents administered in the body to combat microbial infections diffuse to cell membranes once solubilized. This process could result in a lower concentration of antibacterial compounds a given

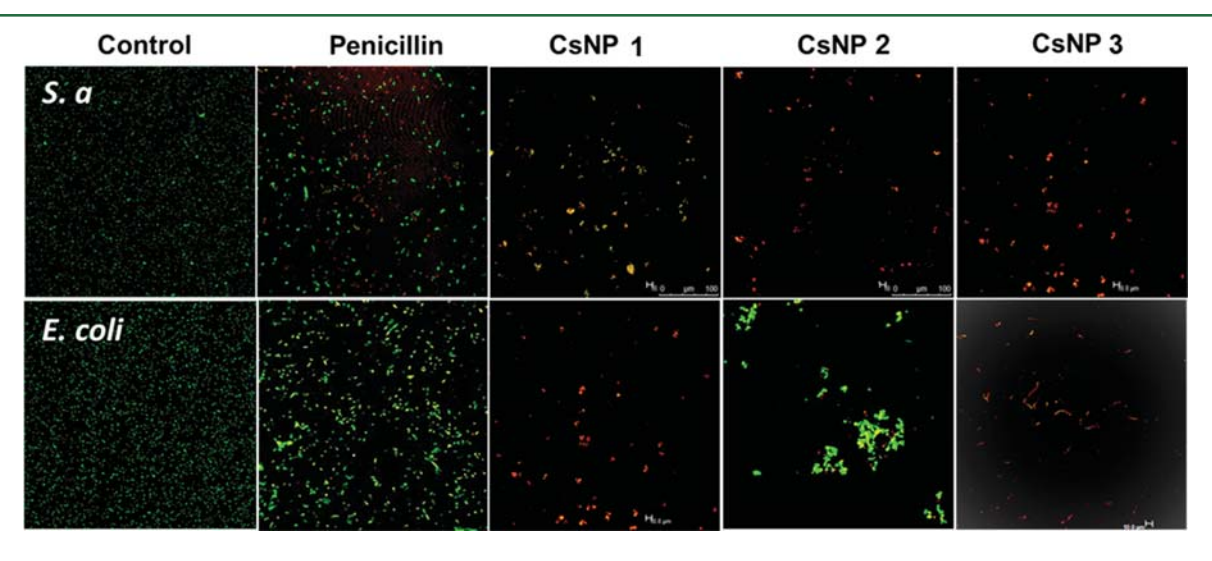


Figure 4. Confocal scanning laser microscopy images of control, penicillin, and CsNP-penicillin conjugates with a concentration of $6 \mu g/mL$ of penicillin (using BacLight live/dead stain, green indicates live cells, red indicates dead cells) against *E. coli* and *S. aureus*. The bacterial solution without CsNPs was used as the control.

Biomacromolecules

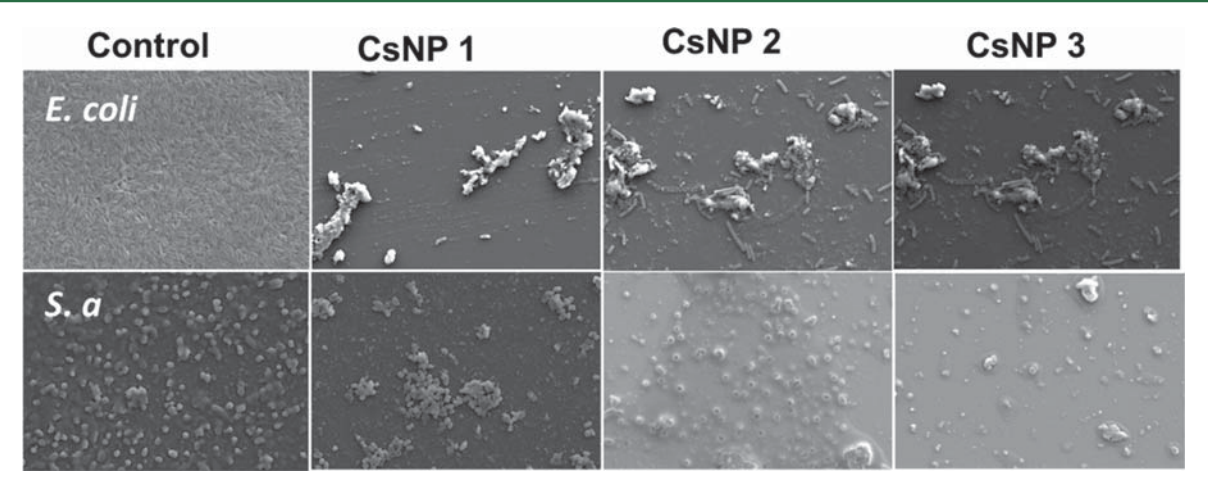


Figure 5. Scanning electron microscopy (SEM) images of control and CsNP-penicillin conjugates with a 6 μ g/mL concentration of penicillin against *E. coli* and *S. aureus*. Bacterial solutions without CsNPs were used as the control.

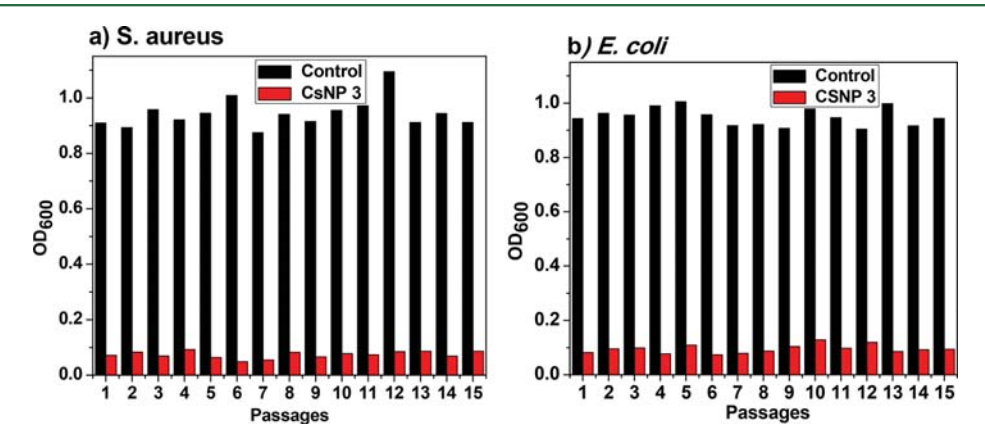


Figure 6. Drug resistance study of CsNP-penicillin conjugates against various bacteria.

bacterial cell receives and thus could be less effective. In contrast, we increased the concentration of the cobaltocenium-penicillin conjugates on the surface, which supplied an enhanced dose to overwhelm the bacterial cell, resulting in effective lysis. In addition, the larger surface area of the nanoparticle could provide more active sites to contact the bacteria resulting in more bacterial death. To determine the toxicity of the CsNPs, we analyzed the cytotoxicity of CsNP 3 on red blood cells (RBCs) by evaluating whether they could lead to hemolysis of RBCs. We found that, even at a concentration as high as 500 μ g/mL, extremely low (<5%) percentages of cells were lysed by CsNP 3 compared to the negative control group as shown in Figure S10. This implies that the CsNPs do not cause significant toxicity and hence could be safe in the host.

CONCLUSIONS

In summary, we engineered the surfaces of silica nanoparticles with cobaltocenium polymers having varied grafting densities using RAFT polymerization. These nanoparticles were then loaded with the β -lactam antibiotic penicillin-G based on electrostatic interactions between the cationic cobaltocenium moiety and anionic antibiotic. The resulting conjugates showed vastly improved bactericidal efficiencies against both Grampositive and Gram-negative bacterial pathogen strains and facilitated the revitalization of the β -lactam drug penicillin. The

nanoparticle-drug complex resisted hydrolysis by β -lactamase, the enzymatic mechanism used by many bacteria to resist β -lactam drugs. Not only did the complex rejuvenate bactericidal efficacy but also provided an enhanced local dose of the penicillin and overwhelmed the bacterial cells, proving to be a more effective antimicrobial agent. This design has enabled us to achieve a promising new paradigm to improve the vitality of conventional antibiotics with strong bactericidal efficacy and minimal cytotoxicity to host human cells.

ASSOCIATED CONTENT

Supporting Information

The Supporting Information is available free of charge on the ACS Publications website at DOI: 10.1021/acs.bio-mac.7b01510.

Synthetic details and characterization data for all of the materials reported here (PDF)

■ AUTHOR INFORMATION

Corresponding Author

*E-mail: tang4@mailbox.sc.edu.

ORCID ®

Parasmani Pageni: 0000-0003-3544-3736 Yucheng Huang: 0000-0002-2367-6199 Brian C. Benicewicz: 0000-0003-4130-1232

Chuanbing Tang: 0000-0002-0242-8241

Notes

The authors declare no competing financial interest.

ACKNOWLEDGMENTS

Research reported in this publication was supported in part by the National Institutes of Health Award #R01AI120987 and the National Science Foundation Award # OIA-1655740.

■ REFERENCES

- (1) van Duin, D.; Paterson, D. L. Multidrug-Resistant Bacteria in the Community: Trends and Lessons Learned. *Infect. Dis. Clin. North Am.* **2016**, *30*, 377–390.
- (2) Courtney, C. M.; Goodman, S. M.; McDaniel, J. A.; Madinger, N. E.; Chatterjee, A.; Nagpal, P. Photoexcited quantum dots for killing multidrug-resistant bacteria. *Nat. Mater.* **2016**, *15*, 529–534.
- (3) García-Quintanilla, M.; Pulido, M. R.; Carretero-Ledesma, M.; McConnell, M. J. Vaccines for Antibiotic-Resistant Bacteria: Possibility or Pipe Dream? *Trends Pharmacol. Sci.* **2016**, *37*, 143–152.
- (4) Mizutani, M.; Palermo, E. F.; Thoma, L. M.; Satoh, K.; Kamigaito, M.; Kuroda, K. Design and Synthesis of Self-Degradable Antibacterial Polymers by Simultaneous Chain- and Step-Growth Radical Copolymerization. *Biomacromolecules* **2012**, *13*, 1554–1563.
- (5) Engler, A. C.; Wiradharma, N.; Ong, Z. Y.; Coady, D. J.; Hedrick, J. L.; Yang, Y.-Y. Emerging trends in macromolecular antimicrobials to fight multi-drug-resistant infections. *Nano Today* **2012**, *7*, 201–222.
- (6) Pu, Y.; Hou, Z.; Khin, M. M.; Zamudio-Vázquez, R.; Poon, K. L.; Duan, H.; Chan-Park, M. B. Synthesis and Antibacterial Study of Sulfobetaine/Quaternary Ammonium-Modified Star-Shaped Poly[2-(dimethylamino)ethyl methacrylate]-Based Copolymers with an Inorganic Core. *Biomacromolecules* **2017**, *18*, 44–55.
- (7) Li, P.; Poon, Y. F.; Li, W.; Zhu, H.-Y.; Yeap, S. H.; Cao, Y.; Qi, X.; Zhou, C.; Lamrani, M.; Beuerman, R. W.; Kang, E.-T.; Mu, Y.; Li, C. M.; Chang, M. W.; Jan Leong, S. S.; Chan-Park, M. B. A polycationic antimicrobial and biocompatible hydrogel with microbe membrane suctioning ability. *Nat. Mater.* **2011**, *10*, 149–156.
- (8) Tew, G. N.; Scott, R. W.; Klein, M. L.; DeGrado, W. F. De Novo Design of Antimicrobial Polymers, Foldamers, and Small Molecules: From Discovery to Practical Applications. *Acc. Chem. Res.* **2010**, *43*, 30–39.
- (9) Ganewatta, M. S.; Tang, C. Controlling macromolecular structures towards effective antimicrobial polymers. *Polymer* **2015**, 63, A1–A29.
- (10) Muñoz-Bonilla, A.; Fernández-García, M. Polymeric materials with antimicrobial activity. *Prog. Polym. Sci.* **2012**, *37*, 281–339.
- (11) Takahashi, H.; Caputo, G. A.; Vemparala, S.; Kuroda, K. Synthetic Random Copolymers as a Molecular Platform To Mimic Host-Defense Antimicrobial Peptides. *Bioconjugate Chem.* **2017**, 28, 1340–1350.
- (12) Abd-El-Aziz, A. S.; Agatemor, C.; Etkin, N. Antimicrobial resistance challenged with metal-based antimicrobial macromolecules. *Biomaterials* **2017**, *118*, 27–50.
- (13) Yan, Y.; Zhang, J.; Ren, L.; Tang, C. Metal-containing and related polymers for biomedical applications. *Chem. Soc. Rev.* **2016**, *45*, 5232–5263.
- (14) Stark, W. J.; Stoessel, P. R.; Wohlleben, W.; Hafner, A. Industrial applications of nanoparticles. *Chem. Soc. Rev.* **2015**, 44, 5793–5805.
- (15) Elsabahy, M.; Wooley, K. L. Design of polymeric nanoparticles for biomedical delivery applications. *Chem. Soc. Rev.* **2012**, *41*, 2545–2561.
- (16) Aruguete, D. M.; Kim, B.; Hochella, M. F.; Ma, Y.; Cheng, Y.; Hoegh, A.; Liu, J.; Pruden, A. Antimicrobial nanotechnology: its potential for the effective management of microbial drug resistance and implications for research needs in microbial nanotoxicology. *Environ. Sci. Process. Impacts* **2013**, *15*, 93–102.
- (17) Richter, A. P.; Brown, J. S.; Bharti, B.; Wang, A.; Gangwal, S.; Houck, K.; Cohen Hubal, E. A.; Paunov, V. N.; Stoyanov, S. D.; Velev,

O. D. An environmentally benign antimicrobial nanoparticle based on a silver-infused lignin core. *Nat. Nanotechnol.* **2015**, *10*, 817–823.

- (18) Sharma, V. K.; Yngard, R. A.; Lin, Y. Silver nanoparticles: Green synthesis and their antimicrobial activities. *Adv. Colloid Interface Sci.* **2009**, *145*, 83–96.
- (19) Rai, M.; Yadav, A.; Gade, A. Silver nanoparticles as a new generation of antimicrobials. *Biotechnol. Adv.* **2009**, *27*, 76–83.
- (20) Li, X.; Robinson, S. M.; Gupta, A.; Saha, K.; Jiang, Z.; Moyano, D. F.; Sahar, A.; Riley, M. A.; Rotello, V. M. Functional Gold Nanoparticles as Potent Antimicrobial Agents against Multi-Drug-Resistant Bacteria. *ACS Nano* **2014**, *8*, 10682–10686.
- (21) Zhao, Y.; Chen, Z.; Chen, Y.; Xu, J.; Li, J.; Jiang, X. Synergy of Non-antibiotic Drugs and Pyrimidinethiol on Gold Nanoparticles against Superbugs. J. Am. Chem. Soc. 2013, 135, 12940–12943.
- (22) Dykman, L.; Khlebtsov, N. Gold nanoparticles in biomedical applications: recent advances and perspectives. *Chem. Soc. Rev.* **2012**, 41, 2256–2282.
- (23) Sirelkhatim, A.; Mahmud, S.; Seeni, A.; Kaus, N. H. M.; Ann, L. C.; Bakhori, S. K. M.; Hasan, H.; Mohamad, D. Review on Zinc Oxide Nanoparticles: Antibacterial Activity and Toxicity Mechanism. *Nano-Micro Lett.* **2015**, *7*, 219–242.
- (24) Raghupathi, K. R.; Koodali, R. T.; Manna, A. C. Size-Dependent Bacterial Growth Inhibition and Mechanism of Antibacterial Activity of Zinc Oxide Nanoparticles. *Langmuir* **2011**, 27, 4020–4028.
- (25) Shi, Y.; Wang, F.; He, J.; Yadav, S.; Wang, H. Titanium dioxide nanoparticles cause apoptosis in BEAS-2B cells through the caspase 8/t-Bid-independent mitochondrial pathway. *Toxicol. Lett.* **2010**, *196*, 21.
- (26) Chen, X.; Mao, S. S. Titanium Dioxide Nanomaterials: Synthesis, Properties, Modifications, and Applications. *Chem. Rev.* **2007**, *107*, 2891–2959.
- (27) Song, J.; Kong, H.; Jang, J. Enhanced antibacterial performance of cationic polymer modified silicananoparticles. *Chem. Commun.* **2009**, 5418–5420.
- (28) Wang, L.; Chen, Y. P.; Miller, K. P.; Cash, B. M.; Jones, S.; Glenn, S.; Benicewicz, B. C.; Decho, A. W. Functionalised nanoparticles complexed with antibiotic efficiently kill MRSA and other bacteria. *Chem. Commun.* **2014**, *50*, 12030–12033.
- (29) Ren, G.; Hu, D.; Cheng, E. W. C.; Vargas-Reus, M. A.; Reip, P.; Allaker, R. P. Characterisation of copper oxide nanoparticles for antimicrobial applications. *Int. J. Antimicrob. Agents* **2009**, *33*, 587–590
- (30) Stoimenov, P. K.; Klinger, R. L.; Marchin, G. L.; Klabunde, K. J. Metal Oxide Nanoparticles as Bactericidal Agents. *Langmuir* **2002**, *18*, 6679–6686.
- (31) Kang, S.; Pinault, M.; Pfefferle, L. D.; Elimelech, M. Single-Walled Carbon Nanotubes Exhibit Strong Antimicrobial Activity. *Langmuir* **2007**, 23, 8670–8673.
- (32) Kang, S.; Herzberg, M.; Rodrigues, D. F.; Elimelech, M. Antibacterial Effects of Carbon Nanotubes: Size Does Matter! *Langmuir* **2008**, *24*, 6409–6413.
- (33) Chen, H.; Wang, B.; Gao, D.; Guan, M.; Zheng, L.; Ouyang, H.; Chai, Z.; Zhao, Y.; Feng, W. Broad-Spectrum Antibacterial Activity of Carbon Nanotubes to Human Gut Bacteria. *Small* **2013**, *9*, 2735–2746.
- (34) Tegos, G. P.; Demidova, T. N.; Arcila-Lopez, D.; Lee, H.; Wharton, T.; Gali, H.; Hamblin, M. R. Cationic Fullerenes Are Effective and Selective Antimicrobial Photosensitizers. *Chem. Biol.* **2005**, *12*, 1127–1135.
- (35) Zou, X.; Zhang, L.; Wang, Z.; Luo, Y. Mechanisms of the Antimicrobial Activities of Graphene Materials. *J. Am. Chem. Soc.* **2016**, 138, 2064–2077.
- (36) Bitar, A.; Ahmad, N. M.; Fessi, H.; Elaissari, A. Silica-based nanoparticles for biomedical applications. *Drug Discovery Today* **2012**, *17*, 1147–1154.
- (37) Tang, F.; Li, L.; Chen, D. Mesoporous Silica Nanoparticles: Synthesis, Biocompatibility and Drug Delivery. *Adv. Mater.* **2012**, *24*, 1504–1534.

(38) Moritz, M.; Geszke-Moritz, M. The newest achievements in synthesis, immobilization and practical applications of antibacterial nanoparticles. *Chem. Eng. J.* **2013**, 228, 596–613.

- (39) Kim, S. H.; Jeyakumar, M.; Katzenellenbogen, J. A. Dual-Mode Fluorophore-Doped Nickel Nitrilotriacetic Acid-Modified Silica Nanoparticles Combine Histidine-Tagged Protein Purification with Site-Specific Fluorophore Labeling. J. Am. Chem. Soc. 2007, 129, 13254—13264.
- (40) Bharali, D. J.; Klejbor, I.; Stachowiak, E. K.; Dutta, P.; Roy, I.; Kaur, N.; Bergey, E. J.; Prasad, P. N.; Stachowiak, M. K. Organically modified silica nanoparticles: A nonviral vector for in vivo gene delivery and expression in the brain. *Proc. Natl. Acad. Sci. U. S. A.* **2005**, *102*, 11539–11544.
- (41) Liu, J.; Levine, A. L.; Mattoon, J. S.; Yamaguchi, M.; Lee, R. J.; Pan, X.; Rosol, T. J. Nanoparticles as image enhancing agents for ultrasonography. *Phys. Med. Biol.* **2006**, *51*, 2179.
- (42) Besinis, A.; De Peralta, T.; Handy, R. D. The antibacterial effects of silver, titanium dioxide and silica dioxide nanoparticles compared to the dental disinfectant chlorhexidine on Streptococcus mutans using a suite of bioassays. *Nanotoxicology* **2014**, *8*, 1–16.
- (43) Sun, T.; Zhang, Y. S.; Pang, B.; Hyun, D. C.; Yang, M.; Xia, Y. Engineered Nanoparticles for Drug Delivery in Cancer Therapy. *Angew. Chem., Int. Ed.* **2014**, 53, 12320–12364.
- (44) Kowalczuk, A.; Trzcinska, R.; Trzebicka, B.; Müller, A. H. E.; Dworak, A.; Tsvetanov, C. B. Loading of polymer nanocarriers: Factors, mechanisms and applications. *Prog. Polym. Sci.* **2014**, *39*, 43–86.
- (45) Elsabahy, M.; Heo, G. S.; Lim, S.-M.; Sun, G.; Wooley, K. L. Polymeric Nanostructures for Imaging and Therapy. *Chem. Rev.* **2015**, *115*, 10967–11011.
- (46) Nederberg, F.; Zhang, Y.; Tan, J. P. K.; Xu, K.; Wang, H.; Yang, C.; Gao, S.; Guo, X. D.; Fukushima, K.; Li, L.; Hedrick, J. L.; Yang, Y.-Y. Biodegradable nanostructures with selective lysis of microbial membranes. *Nat. Chem.* **2011**, *3*, 409–414.
- (47) Zhang, J.; Chen, Y. P.; Miller, K. P.; Ganewatta, M. S.; Bam, M.; Yan, Y.; Nagarkatti, M.; Decho, A. W.; Tang, C. Antimicrobial Metallopolymers and Their Bioconjugates with Conventional Antibiotics against Multidrug-Resistant Bacteria. *J. Am. Chem. Soc.* **2014**, *136*, 4873–4876.
- (48) Yang, P.; Bam, M.; Pageni, P.; Zhu, T.; Chen, Y. P.; Nagarkatti, M.; Decho, A. W.; Tang, C. Trio Act of Boronolectin with Antibiotic-Metal Complexed Macromolecules toward Broad-Spectrum Antimicrobial Efficacy. *ACS Infect. Dis.* **2017**, *3*, 845–853.
- (49) Zhang, J.; Yan, J.; Pageni, P.; Yan, Y.; Wirth, A.; Chen, Y.-P.; Qiao, Y.; Wang, Q.; Decho, A. W.; Tang, C. Anion-Responsive Metallopolymer Hydrogels for Healthcare Applications. *Sci. Rep.* **2015**, *5*, 11914.
- (50) Li, C.; Han, J.; Ryu, C. Y.; Benicewicz, B. C. A Versatile Method To Prepare RAFT Agent Anchored Substrates and the Preparation of PMMA Grafted Nanoparticles. *Macromolecules* **2006**, *39*, 3175–3183.
- (51) Zhang, J.; Yan, Y.; Chance, M. W.; Chen, J.; Hayat, J.; Ma, S.; Tang, C. Charged Metallopolymers as Universal Precursors for Versatile Cobalt Materials. *Angew. Chem., Int. Ed.* **2013**, 52, 13387–13391.
- (52) Bauer, A.; Kirby, W.; Sherris, J. C.; Turck, M. Antibiotic susceptibility testing by a standardized single disk method. *Am. J. Clin. Pathol.* **1966**, *45*, 493.
- (53) Ren, L.; Hardy, C. G.; Tang, C. Synthesis and Solution Self-Assembly of Side-Chain Cobaltocenium-Containing Block Copolymers. J. Am. Chem. Soc. 2010, 132, 8874–8875.
- (54) Zhang, J.; Ren, L.; Hardy, C. G.; Tang, C. Cobaltocenium-Containing Methacrylate Homopolymers, Block Copolymers, and Heterobimetallic Polymers via RAFT Polymerization. *Macromolecules* **2012**, *45*, 6857–6863.
- (55) Zhang, J.; Yan, Y.; Chen, J.; Chance, W. M.; Hayat, J.; Gai, Z.; Tang, C. Nanostructured Metal/Carbon Composites from Heterobimetallic Block Copolymers with Controlled Magnetic Properties. *Chem. Mater.* **2014**, *26*, 3185–3190.

- (56) Moad, G.; Rizzardo, E.; Thang, S. H. Radical addition–fragmentation chemistry in polymer synthesis. *Polymer* **2008**, *49*, 1079–1131.
- (57) Chiefari, J.; Chong, Y.; Ercole, F.; Krstina, J.; Jeffery, J.; Le, T. P.; Mayadunne, R. T.; Meijs, G. F.; Moad, C. L.; Moad, G.; Rizzardo, E.; Thang, S. H. Living free-radical polymerization by reversible addition–fragmentation chain transfer: the RAFT process. *Macromolecules* **1998**, 31, 5559–5562.
- (58) Boyer, C.; Bulmus, V.; Davis, T. P.; Ladmiral, V.; Liu, J.; Perrier, S. Bioapplications of RAFT polymerization. *Chem. Rev.* **2009**, *109*, 5402–5436.
- (59) Li, Y.; Benicewicz, B. C. Functionalization of silica nanoparticles via the combination of surface-initiated RAFT polymerization and click reactions. *Macromolecules* **2008**, *41*, 7986–7992.
- (60) Bao, C.; Tang, S.; Horton, J. M.; Jiang, X.; Tang, P.; Qiu, F.; Zhu, L.; Zhao, B. Effect of Overall Grafting Density on Microphase Separation of Mixed Homopolymer Brushes Synthesized from Y-Initiator-Functionalized Silica Particles. *Macromolecules* **2012**, 45, 8027–8036.
- (61) Kumar, S. K.; Jouault, N.; Benicewicz, B.; Neely, T. Nanocomposites with polymer grafted nanoparticles. *Macromolecules* **2013**, *46*, 3199–3214.
- (62) Wiegand, I.; Hilpert, K.; Hancock, R. E. W. Agar and broth dilution methods to determine the minimal inhibitory concentration (MIC) of antimicrobial substances. *Nat. Protoc.* **2008**, *3*, 163–175.
- (63) Pendleton, J. N.; Gorman, S. P.; Gilmore, B. F. Clinical relevance of the ESKAPE pathogens. *Expert Rev. Anti-Infect. Ther.* **2013**, *11*, 297–308.
- (64) O'Callaghan, C. H.; Morris, A.; Kirby, S. M.; Shingler, A. H. Novel Method for Detection of β -Lactamases by Using a Chromogenic Cephalosporin Substrate. *Antimicrob. Agents Chemother.* **1972**, *1*, 283–288.